RESEARCH

Multiparametric arterial spin-labeling and diffusion-weighted imaging of phenotyping of polycystic ovaries

Heba M. Abou El-Atta[1], Khaled Abdel Baky[2*], Mahmoud Thabet[3] and Mona Talaat[4]

Abstract

Background Polycystic ovarian syndrome [PCO] is a worldwide endocrine disorder affecting women of reproductive age. Diagnosis and differentiation of PCO phenotypes are crucial for disease prognosis, fertility outcome, and treatment planning. This study aims to assess arterial spin labeling perfusion (ASL) and diffusion-weighted imaging (DWI) derived metrics in the diagnosis of PCO, differentiation of its phenotypes, and correlation of these metrics with laboratory measurements.

Results ASL and DWI of the pelvis were performed on 72 PCO patients and another 20 age-matched control group. Two observers measured the blood flow (BF) and ADC in the ovarian stroma. Serum levels of testosterone, dehydroepiandrosterone sulfate (DHEAS), and body mass index (BMI) were calculated. BF values were significantly higher in PCO patients than in control cases ($P = 0.001$), with area under the curve (AUC) of (0.94 and 0.89) and accuracy of (96% and 92%) for both observers, respectively. Also, BF values were significantly higher in classic than in non-classic PCO cases ($P = 0.001$), with AUC of (0.92 and 0.90) and accuracy of (91%) for both observers, respectively. ADC values were significantly lower in PCO patients than in control cases ($P = 0.001$), with AUC of (0.85 and 0.84) for the first observer and second observer, respectively. ADC values were significantly lower in classic PCO patients than in non-classic patients ($P = 0.001$), with AUC of (0.85 and 0.84) and accuracy of (77% and 81%) for both observers, respectively. Combined values of BF and ADC showed an accuracy of 91% and 86% for differentiating patient from control cases for both observers, respectively, and an accuracy of 92% for differentiating classic from non-classic PCO phenotypes. A significant correlation was found between ADC, BF metrics, and both serum testosterone and DHEAS levels ($P < 0.05$).

Conclusions Combination of ASL and ADC can be used in PCO diagnosis and can help in the differentiation of its phenotypes. Serum levels of testosterone and DHEAS have a significant correlation with ADC and BF metrics.

Keywords Ultrasound, Ovary, Polycystic, Phenotypes

*Correspondence:
Khaled Abdel Baky
dr_khaledrad@yahoo.com
Full list of author information is available at the end of the article

El-Atta *et al. Egypt J Radiol Nucl Med*   (2024) 55:62

Page 2 of 10

Background

Polycystic ovarian syndrome [PCO] is a global complex endocrine disorder in women of reproductive age [1]. The hallmarks of the disease include menstrual disturbances, multiple ovarian cysts, and excess androgen. Women suffer from acne, hirsutism, the inability to conceive, and obesity. They also have high serum levels of free testosterone [T], androstenedione, dehydroepiandrosterone sulfate [DHEAS], luteinizing hormone [LH], and the LH/FSH ratio. The high serum level of anti-Mullerian hormone [AMH] is used as a marker for the increased total number of ovarian follicles, thus reflecting the severity of PCO. The metabolic aspects of PCO include obesity, insulin resistance, and diabetes mellitus type II. In addition, there is an increased risk of endometrial hyperplasia, cardiovascular diseases, and cerebrovascular disorders [2–6]. According to the presence of oligo-anovulation [O], clinical or biochemical signs of hyperandrogenism [HA], and polycystic ovarian morphology [PCOM], the National Institute of Health [NIH] in 2012 classified PCO into four phenotypes (A, B, C, and D). Phenotype A includes [O+HA+PCOM], phenotype B includes [O+HA], phenotype C includes [HA+PCOM], and phenotype D includes [O+PCOM]. The classic PCO [phenotype A/B] is manifested by more obvious menstrual dysfunction, hyperandrogenism, an abnormal lipid profile, and an increased body mass index. Furthermore, there is an elevated level of insulin and anti-Mullerian hormones, with an increased risk of other complications. However, the non-classic PCO is associated with less endocrine and metabolic dysfunction and a lower incidence of complications [7–12].

Hyperandrogenism has an essential role in the pathogenesis of PCO. High testosterone levels are associated with excess abdominal fat, obesity, and a higher risk of insulin resistance. Moreover, in both animal models and women with PCO, excess androgen leads to PCO morphology and ovulatory dysfunction [6, 7]. The Endocrine Society recommends using elevated total, bioavailable, or free serum testosterone levels in the diagnosis of PCO. However, O'Reilly et al. [13] reported that a high androstenedione level is associated with an excess of testosterone. They also suggested that measuring serum testosterone and androstenedione is a good predictor of metabolic risk in PCO. Patients with adrenal hyperandrogenism and elevated DHEAS have a better metabolic profile than patients with ovarian hyperandrogenism and elevated free testosterone. In PCO women, a high DHEAS/free testosterone or DHEAS/total testosterone ratio is associated with a favorable metabolic phenotype [14].

The distinction between different PCO phenotypes is crucial for disease severity prognosis, the outcome of fertility, and treatment planning. The role of ultrasound (US) in PCO diagnosis, including transabdominal and transvaginal US, is discussed in various studies, depending mainly on morphologic changes, ovarian volume, and the number of follicles [15–24]. Magnetic resonance imaging (MRI) is a valuable alternative for assessing follicular characteristics and ovarian morphology in PCO patients. MRI is a noninvasive imaging modality that has excellent anatomic resolution and is not affected by surrounding fat thickness in comparison with the US, especially in obese patients [25, 26]. Diffusion-weighted imaging (DWI) is a noninvasive technique that measures the water movement in the extracellular space. Hypercellularity, or an increased nuclear-to-cytoplasmic ratio, limits water diffusivity. The apparent diffusion coefficient (ADC) is a measure of biological tissue's specific diffusion capacity [27, 28]. Arterial spin labeling (ASL) is an MRI technique that vests the noninvasive measurement of perfusion at the tissue level. Ovarian enhancement and perfusion vary according to hormone status and the phase of the menstrual cycle. Currently, ASL is known to be helpful in cerebral blood flow evaluation, but the assessment of pelvic organs' blood flow by ASL is not yet known [29, 30]. To the best of our knowledge, there is no prior research in English literature to assess the use of ASL with DWI in PCO phenotyping.

The purpose of this work is to determine the effectiveness of ASL and DWI metrics in PCO diagnosis and differentiation between its different phenotypes, as well as correlating these metrics with laboratory measurements.

Methods

Subjects

Ethical approval of this prospective study was obtained from the local institutional review board. All patients provided their written informed consent. The study included patients who met the Rotterdam criteria [31] and underwent TVS, having disturbed menstruation, hirsutism, and/or infertility. Seventy-two patients fulfilled the inclusion criteria of our study, out of the 76 patients initially diagnosed with PCO based on the Rotterdam criteria [31]. The four excluded patients had a dominant follicle larger than 10 mm and bad imaging quality. The remaining 72 patients aged 23–43 years old. The patients were categorized into classic phenotypes, included type I ($n=36$) and type II ($n=10$), and non-classic form, which included type III ($n=16$) and type IV ($n=10$). Serum levels of testosterone and DHEAS were measured for all cases. The body mass index (BMI) was calculated for each case. Another 20-age-matched control group, aged 20–42 years, underwent ASL and DWI of the pelvis as well as measurement of serum levels of testosterone and BMI calculation.

El-Atta *et al. Egypt J Radiol Nucl Med*   (2024) 55:62

Page 3 of 10

MR imaging

The procedure of MR examination was explained to the patient. Patients fast for 4–6 h. Before MR imaging, an intravenous injection of 10 mg of an antispasmodic drug (Visceralgine) was given to reduce bowel peristalsis, particularly for diffusion-weighted imaging. MRI was done during the early follicular phase (about the 5th–6th days of the menstrual cycle). MR imaging was performed on a 1.5-T MR imaging unit (Ingenia, Philips, the Netherlands). All the patients were imaged in the supine position, head first, using a pelvic phased-array coil (Table 1).

ASL perfusion imaging was performed with a pseudo-continuous labeling technique. A single time point obtained after the labeling pulse with fast spin-echo single-shot echo-planar imaging parallels sequence. The positioning of the labeling pulse covered both ovarian arteries, and the post-labeling delay was 1.5 s. The parameters used were: repetition time/echo time 3600/5.9 ms, echo train length 21, matrix 128×96, FOV 240×240 mm2, imaging/tagging slice thickness 10/200 mm. The imaging of each inversion time was in 90 s.

Image analysis

The analysis of images was done blindly by two expert radiologists in female imaging over 15 and 10 years, respectively. In ASL imaging, the post-processing of arterial spin-tagging data includes initial subtraction of alternating tag and control image pairs, motion correction, and generating ASL gray-scale and colored maps. Regions of interest (ROIs) are manually positioned in the ovarian high-signal area within the ovarian stroma. Both regions' ROIs were comparable in size, with a range of 0.25 to 2.0 cm^2. Images were compared with other conventional MR images to avoid follicles. In DWI, the application of matched ADC maps was done using functional tool software from Phillips Advantage windows Workstation. ADC values were measured by manual placement of ROIs of similar size and location within the stroma of both ovaries. Images were compared also with other conventional MR images to avoid follicles.

Statistical analysis

The IBM SPSS software package version 20.0 was used to analyze the data. Numbers and percentages were used to describe the qualitative data. Measures of quantitative data included mean, standard deviation, and range (minimum and maximum) after testing normality using the Shapiro–Wilk test. The significance of the obtained results was judged at the 5% level. All tests were two-tailed. The tests used were: Student t test (for quantitative parametric variables, to compare between different groups), the ROC curve (for detection of validity and cut-off point in comparison with sure diagnostic test), validity indices (sensitivity, specificity, accuracy), and lastly, binary logistic regression was used to detect the probability of combined variables in the prediction of cases with ROC curve application for saved probabilities.

Results

Seventy-two patients fulfilled the inclusion criteria of our study, out of the 76 patients initially diagnosed with PCO based on the Rotterdam criteria [31]. The four excluded patients had a dominant follicle larger than 10 mm and bad imaging quality. The remaining 72 patients aged 23–43 years old. The patients were classified into classic phenotypes, including type I ($n=36$) and type II ($n=10$) (Fig. 1, 2), and non-classic form, including type III ($n=16$) and type IV ($n=10$). The other control group included 20 females aged 20–42 years. Demographic details are provided (Table 2).

The mean BF values of ovarian stroma in PCO patients were (722 ± 114 and 723 ± 114 mL/100 g/min) and in control were (510 ± 79 and 539 ± 11 mL/100 g/min) by first and second observers, respectively, with a significant difference ($P = 0.001$). Selection of (510.38 and 514.73 mL/100 g/min) as a threshold value of BF of

Table 1 The sequences used in the study are listed in the following table

Sequence	TR (m sec.)	TE (m sec.)	FOV (mm)	Matrix	Slice thickness (mm)	Slice gap (mm)
T2 sagittal	3000	90	290×290	208×205	4	1.5
T2 axial	3300	100	288×350	292×180	6	1.3
T1 axial	500	10	260×216	263×171	6	1.3
T1 SPAIR axial	530	8	240×240	240×190	6	1.3
DWI (b: 0, 500, 1000, 1500)	5000	77	240×240	124×100	6	1
T2 coronal	5000	90	300×300	272×200	5.5	1
T1 axial post-contrast	500	10	260×216	263×171	6	1.3
T1 coronal post-contrast	420	10	280×280	256×220	6	1

TR Repetition Time, *TE* Time to echo, *FOV* Field of view, *SPAIR* Spectral Adiabatic Inversion Recovery, *DWI* Diffusion-weighted imaging
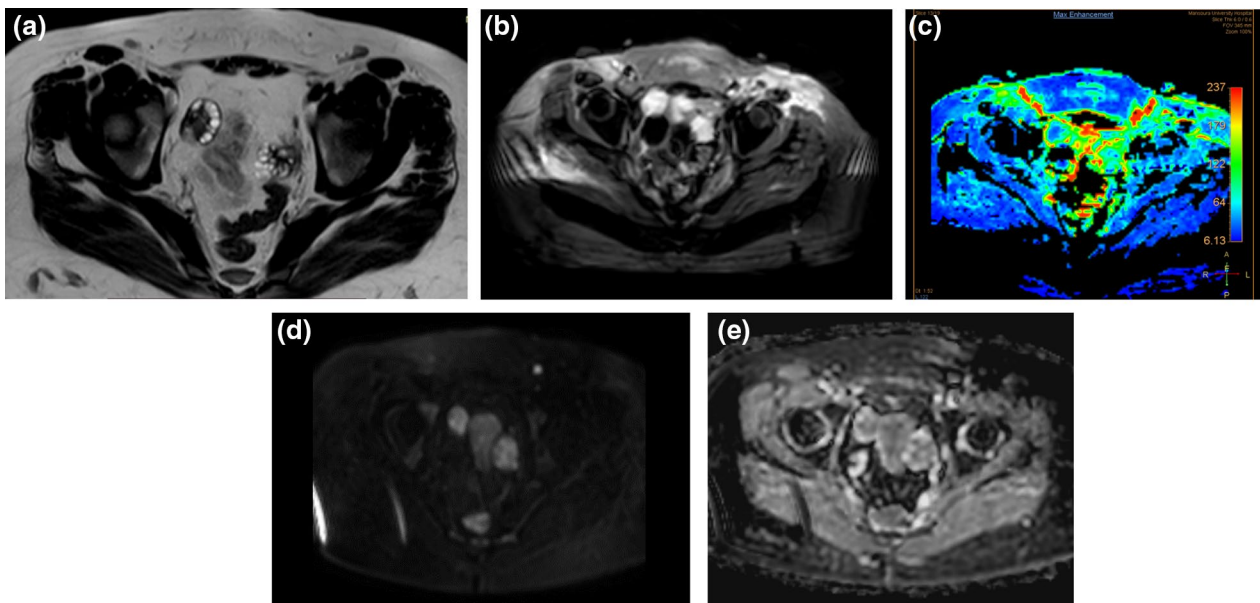
Fig. 1 Classic Polycystic ovaries: A 26-year-old female with PCO **A** Axial T2-weighted image shows high signal small uniform peripherally arranged follicles, while the central stroma is of comparatively low T2. **B**, **C** ASL blood flow gray scale map **B** colored scale **C** show high signal intensity within ovarian stroma parts are 790.13, 812.02 mL/100 g/min for right and left sides, respectively. **D** and **E** DWI and ADC map show high signal of ovarian stoma on DWI image **D** with ADC values of ovarian stroma are 1.091, 1.012 × 10⁻³ mm²/s for right and left sides, respectively
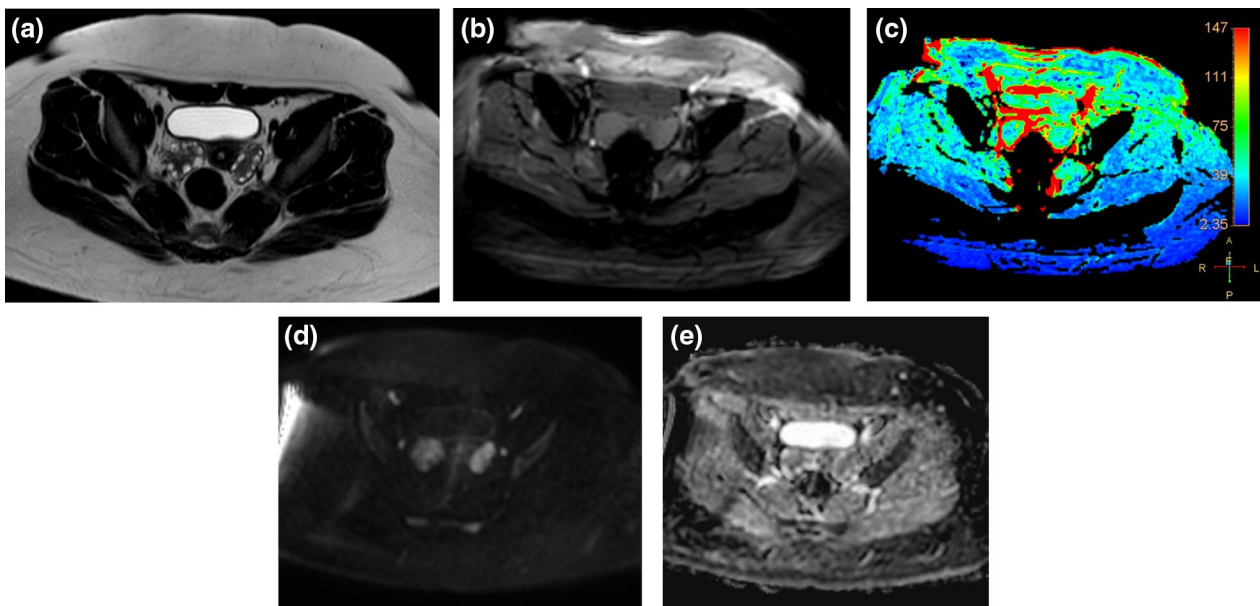

Fig. 2 Non-classic Polycystic ovaries: A 22 years old female with PCO **A** Axial T2-weighted image shows high signal small uniform peripherally arranged follicles, while the central stroma is of comparatively low T2 **B** and **C** ASL blood flow gray scale map **B** colored scale **C** show high signal intensity within ovarian stroma are 720.45, 690.28 mL/100 g/min for right and left sides, respectively. **D** and **E** DWI and ADC map show high signal of ovarian stoma on DWI image **D** with ADC values of ovarian stoma are 1.301, 1.35 × 10⁻³ mm²/s for right and left sides, respectively

ovarian stroma used for diagnosis of PCO revealed AUC of 0.94 and 0.89, accuracy of 96% and 92%, sensitivity of 98% and 95%, specificity of 90% and 80% by first and second observers, respectively. The mean ADC values of ovarian stoma in PCO patients were (1.20 ± 0.37 and $1.16 \pm 0.34 \times 10^{-3}$ mm²/s) and in control females were

El-Atta *et al. Egypt J Radiol Nucl Med*   (2024) 55:62

Page 5 of 10

Table 2 Demographic and laboratory data of patients and control groups

	Classic (*n* = 46)	Non-classic (*n* = 26)	Control (*n* = 20)	Test of significance
Age	23–38 Mean = 27.04	25–43 Mean = 27.6	20–42 Mean = 28.2	
BMI	26.33 ± 2.65	25.48 ± 2.77	22.35 ± 3.69	$F = 12.90$ $P < 0.001$*
DHEAS	342.33 ± 85.47	297.65 ± 109.55		$t = 1.92$ $p = 0.059$
Testosterone	90.50 ± 10.09	56.73 ± 24.84	32.0 ± 13.87	$F = 98.72$ $P < 0.001$*

BMI Body mass index, *DHEAS* Dehydroepiandrosterone sulfate. *indicates significant difference

Table 3 Mean and SD of BF, ADC of PCO and controls

	Control *n* = 20	Patients *n* = 72	Test of significance
ADC (First observer)	1.66 ± 0.14	1.20 ± 0.37	0.001
ADC (second observer)	1.61 ± 0.23	1.16 ± 0.34	0.001
BF (First observer)	510.02 ± 79.21	722.25 ± 114.77	0.001
BF (second observer)	539.07 ± 111.26	723.29 ± 114.35	0.001

SD standard deviation, *ADC* apparent diffusion coefficient, *BF* blood flow

(1.66 ± 0.14 and $1.61 \pm 0.23 \times 10^{-3}$ mm^2/s) for first and second observers, respectively, and a significant difference was observed ($P = 0.001$). Selection of (1.57 and 1.54×10^{-3} mm^2/s) as a threshold of ADC of ovarian stroma for diagnosis of PCO yielded AUC of 0.85 and 0.84, accuracy of 79% and 80%, sensitivity of 80% and 81%, specificity of 75% and 75% for the first and second observers, respectively (Table 3). Combined use of BF and ADC of ovarian stroma in the diagnosis of PCO yielded AUC of (0.94 and 0.90), accuracy of (91% and 86%), sensitivity of (91% and 90%), and specificity of (90% and 75%) for the first and second observers, respectively (Table 4) and (Fig. 3).

The mean BF values of the stroma in classic PCO patients were (790 ± 47 and 790 ± 46.88 mL/100 g/min) and of non-classic PCO patients were (601 ± 97 and

604 ± 100 mL/100 g/min) for first and second observers, respectively, with a significant difference ($P = 0.001$). Selection of (689 and 702.5 mL/100 g/min) as a threshold value of BF of ovarian stroma used for differentiation of classic from non-classic PCO yielded AUC of 0.921 and 0.908, accuracy of 91% and 91%, sensitivity of 98% and 96%, and specificity of 81% and 85% for the first and second observers, respectively. The mean ADC values of ovarian stoma in classic PCO patients were (1 ± 0.32 and $1 \pm 0.27 \times 10^{-3}$ mm^2/s) and non-classic PCO patients (1.5 ± 0.3 and $1.4 \pm 0.3 \times 10^{-3}$ mm^2/s) for the first and second observers, respectively, with a significant difference ($P = 0.001$). Selection of (1.4 and 1.3×10^{-3} mm^2/s) as a threshold value of ADC of ovarian stroma for differentiation of a classic from non-classic PCO revealed AUC of 0.85 and 0.84, accuracy of 77% and 81%, sensitivity of 84% and 91%, and specificity of 69% and 65% for the first and second observers, respectively (Table 5). Combined use of BF and ADC of ovarian stroma in differentiating classic from non-classic PCO revealed AUC of (0.956 and 0.957), accuracy of (91% and 91%), sensitivity of (97% and 93%), and specificity of (80% and 88%) for first and second observers, respectively (Table 6) and (Fig. 4).

There is no significant difference between classic and non-classic types when using DHEAS as a reference ($P = 0.059$). There was a significant difference between the classic, non-classic, and control groups when using

Table 4 ROC curve of BF and ADC of PCO patients and control

	AUC	*P* value	Cut-off point	Sensitivity (%)	Specificity (%)	Accuracy (%)
Patients versus controls						
ADC (First observer)	0.853	0.001	1.57	80	75	79
ADC (second observer)	0.844	0.001	1.54	81	75	80
BF (First observer)	0.948	0.001	510.38	98	90	96
BF (second observer)	0.894	0.001	514.73	95	80	92
Combined (first observer)	0.945	0.001		91	90	91
Combined (second observer)	0.903	0.001		90	75	86

ROC Receiver operating characteristic, *AUC* area under the curve, *ADC* apparent diffusion coefficient, *BF* blood flow

El-Atta *et al. Egypt J Radiol Nucl Med*   (2024) 55:62
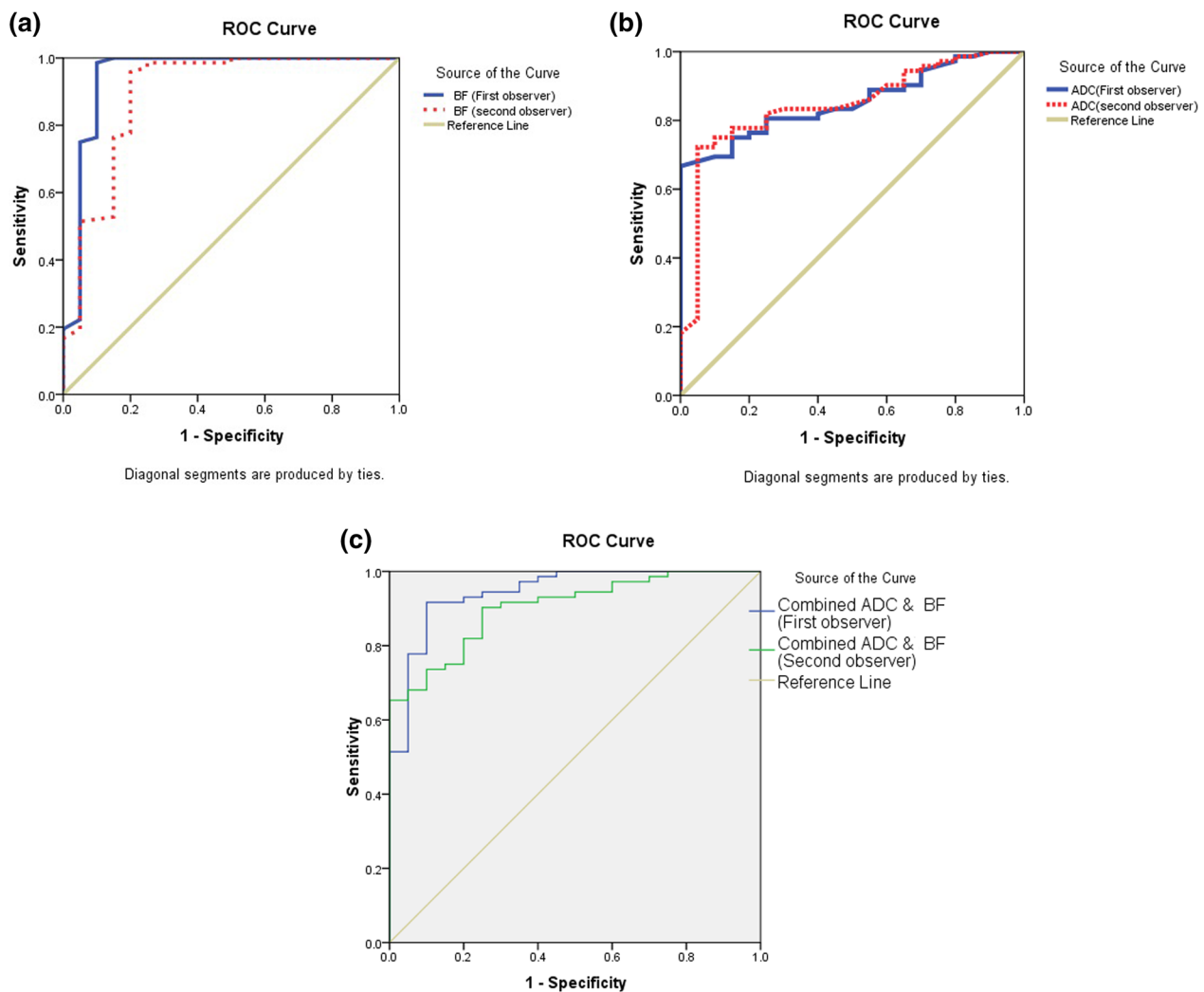
Page 6 of 10

Fig. 3 ROC of BF, ADC, and combined parameters in patients versus controls: **A** BF = 0.95 and 0.89 in first and second observers, respectively **B** ADC = 0.85 and 0.84 in first and second observers, respectively. **C** Combined = 0.95 and 0.90 in first observer and second observers, respectively

Table 5 Mean and SD of BF and ADC of PCO phenotypes

	Classic *n* = 46	Non-Classic *n* = 26	test of significance
ADC (First observer)	1.03 ± 0.31	1.49 ± 0.28	0.001
ADC (second observer)	1.007 ± 0.26	1.434 ± 0.31	0.001
BF (First observer)	790.81 ± 47.02	600.93 ± 97.33	0.001
BF (second observer)	790.59 ± 46.88	604.20 ± 100.48	0.001

SD standard deviation, *ADC* apparent diffusion coefficient, *BF* blood flow

testosterone as an indicator ($P = 0.001$). Also, BMI exhibits significant variability between the three groups ($P < 0.001$) (Table 2).

The relationship between MRI-derived parameters and laboratory findings showed a significant negative correlation between ADC and both serum testosterone and DHEAS levels ($P = 0.001$) for both observers. However, a non-significant negative correlation between ADC and BMI was noticed for the second observer. The relation between BF and both serum testosterone and DHEAS levels showed a significant positive correlation ($P < 0.05$). However, a non-significant positive correlation between BF and BMI was noticed for both observers.

Discussion

In the present study, we aimed to evaluate the feasibility and reproducibility of ASL technique in the assessment of ovarian blood flow in patients with polycystic ovaries. Studying vascular changes in the ovaries of PCO women may allow us to gain further insights into the underlying

El-Atta *et al. Egypt J Radiol Nucl Med*   (2024) 55:62

Page 7 of 10

Table 6 ROC curve of BF and ADC of PCO classic and non-classic phenotypes

	AUC	P value	Cutoff point	Sensitivity (%)	Specificity (%)	Accuracy (%)
ADC (First observer)	0.858	0.001	1.43	84	69	77
ADC (second observer)	0.847	0.001	1.34	91	65	81
BF (First observer)	0.921	0.001	688.75	97	80	91
BF (second observer)	0.908	0.001	702.51	95	84	91
Combined (first observer)	0.956	0.001		97	80	91
Combined (second observer)	0.957	0.001		93	88	91

ROC Receiver operating characteristic, *AUC* area under the curve, *ADC* apparent diffusion coefficient, *BF* blood flow
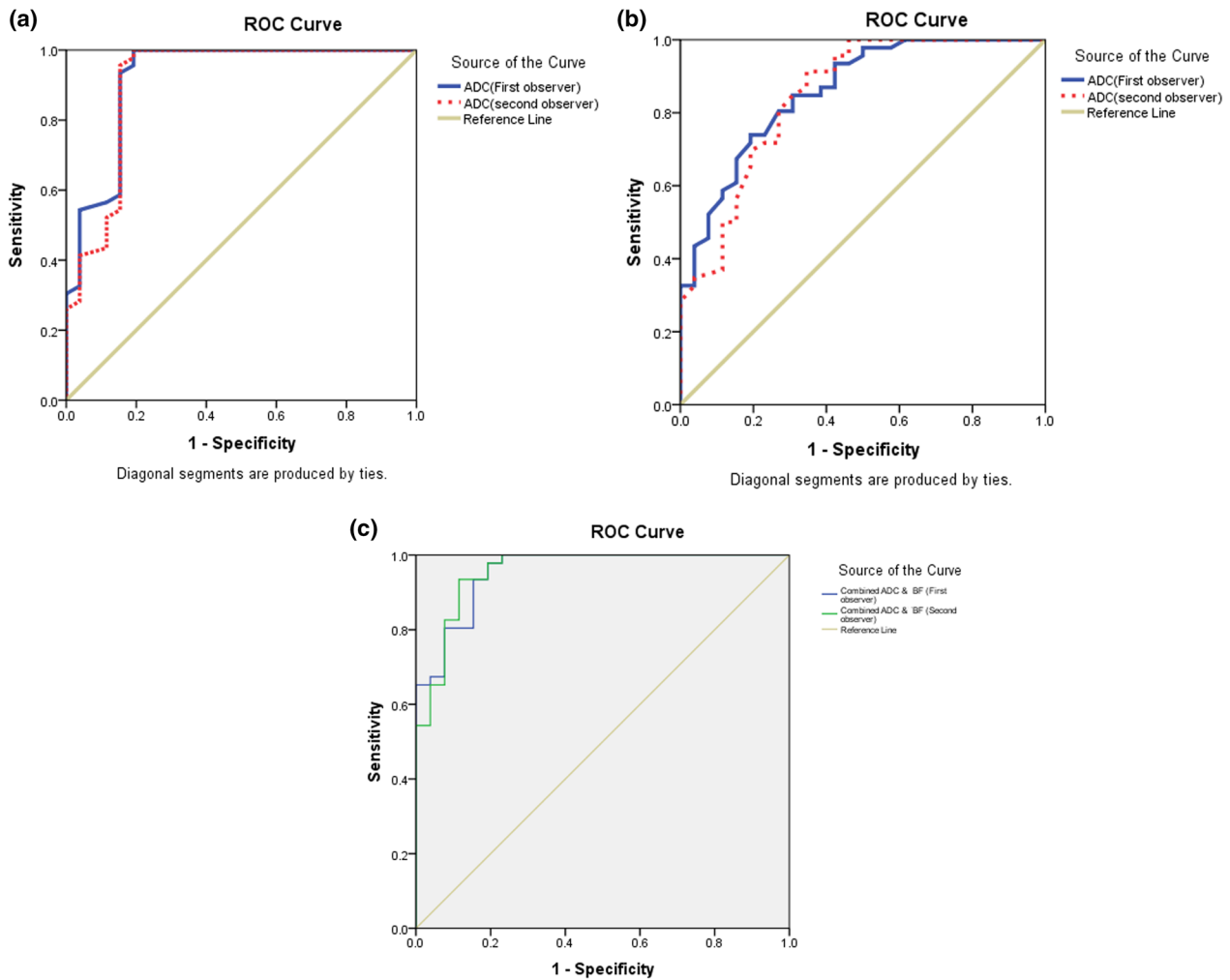

Fig. 4 ROC of BF, ADC and combined parameters in classic versus non-classic: **A** BF = 0.92 in first observer and 0.91 in the second observer **B** ADC = 0.86 in first observer and 0.85 in second observer **C** combined = 0.95 in both observers

pathophysiology of the disease. ASL blood flow measurements can help in PCO identification and phenotypic differentiation.

Studies on ASL measurement have been focused on the brain thus far [29, 30]. But, to the best of our knowledge, no studies have been done on the application of ASL in

PCO patient evaluation. Our study demonstrated that ovarian stroma in PCO patients exhibits significantly higher blood flow ($P = 0.001$) compared to control cases. A recent study used an intravoxel incoherent motion (IVIM) MRI model to assess both Brownian water diffusion and microcapillary perfusion separately in PCO

El-Atta *et al. Egypt J Radiol Nucl Med*   (2024) 55:62

Page 8 of 10

patients and control groups. They found high values of pseudo-diffusion coefficient (D*) and perfusion fraction (*f*) in PCO patients, indicating increased stromal ovarian vascularity [32].

Other studies using Doppler ultrasound stated that in cases of PCO, there's ovarian stromal hyperemia with lower arterial Pulsatility Index (PI) and Resistive Index values (RI). The reduced PI and RI values suggest the increased number and dilatation of ovarian stromal vessels in PCO [33, 34]. In accordance with our results, another study examined the mean signal intensity-time curve and found that PCO patients demonstrated greater and more rapid ovarian enhancement and wash-out. This enhancement behavior on the DCE-MR imaging examination may differ significantly from that of control subjects [35, 36].

As observed in this study, ADC values were lower in patients with PCO compared to control cases ($P=0.001$). These results are comparable to a similar study that concluded that ADC measurements of the ovarian stroma are lower in patients with PCO than in control subjects ($P=0.001$) and this might help improve the diagnosis of PCO [27, 28, 32]. Reduced diffusivity, in general, is related to increased cellularity, increased cell size, or microcirculation, which was discussed in many studies before [37–39]. According to a study by Papachroni et al. [40], the ovarian stroma of PCO cases may have lower ADC values due to the abnormal deposition of excess collagen in the polycystic ovarian stroma. Other studies attributed the decrease in ADC value to high levels of vascular endothelial growth factor (VEGF) that have been detected in the stroma of polycystic ovaries [40, 41]. Similar findings of reduced ADC values and increased levels of VEGF were found in hepatocellular carcinoma [42].

Phenotype differentiation in cases of PCO is essential for management, assessment of disease severity, and complication prognosis. This depends mainly on clinical, laboratory data, and ovarian morphology on ultrasound. In this study, we study the role of ASL and DWI metrics in the differentiation of classic and non-classic phenotypes of PCO. Our study results showed that ASL blood flow-derived metrics showed higher values in classic phenotypes (A and B) compared to non-classic types (C and D) ($P=0.001$), while ADC values were lower in classic than non-classic cases ($P=0.001$). This may be attributed to increased ovarian stroma and vascularity in classic than non-classic PCO cases. A study using ultrasound for phenotype differentiation revealed that the ovarian volume differed significantly between classic and non-classic phenotypes of PCO, with an accuracy of 75% [10].

The combined values of ASL blood flow and ADC of the ovarian stroma in the present study have shown a high significant difference between PCO cases and control cases. A study by Ozkok et al. [32] also found significantly reduced ADC values and increased IVIM MRI-derived perfusion parameters in PCO patients**.** The combined use of ASL blood flow and ADC of the ovarian stroma also found a highly significant difference between classic and non-classic PCO phenotypes. This will add great value to phenotype differentiation by MR imaging, which, as far as we know, has not been discussed before in English literature.

Our results revealed that there is a significant difference in testosterone level and BMI between the classic, non-classic, and control groups ($P=0.001$). While the level of DHEAS was non-significant in differentiation between classic and non-classic phenotypes ($P=0.059$). Our results showed agreement with Yuan et al. [14], who reported that there is a highly significant correlation between testosterone and BMI with different phenotype groups of PCO. On the other hand, there is partial agreement with O'Reilly et al. [13], who reported a positive correlation between high testosterone and PCO, and disagreement with our results regarding BMI.

Significant increase in levels of testosterone and DHEAS was associated with reduced ADC and increased BF in PCO patients. Other studies also found a significant correlation between Doppler indices and laboratory ovarian dysfunction markers [33, 43]**.** The correlation between imaging and laboratory biomarkers would prove the reliability of using these markers as predictors for PCO.

This study has a number of limitations. First, it included a relatively small number of patients. Further research in a larger cohort is recommended. Second, a 1.5-T scanner was used in this study. It is advised that further studies be done on 3-T machines for better assessment. Third, ASL results could be impacted by the degree of arterial stenosis; further studies are required using multi-parametric MR imaging combined with contrast MR angiography [36, 44] to evaluate arterial stenosis in future.

Conclusions

We came to the conclusion that PCO diagnosis and differentiation between its phenotypes can be aided by combining ASL and DWI-derived metrics of ovarian stroma. A significant correlation between those imaging metrics and serum levels of testosterone and DHEAS supports the use of ASL and DWI in the evaluation of PCO.

Abbreviations

BF	Blood flow
BMI	Body mass index
PCO	Polycystic ovaries
ASL	Arterial spin labeling
ADC	Apparent diffusion coefficient
DWI	Diffusion-weighted imaging
DHEAS	Dehydroepiandrosterone sulfate
AUC	Area under the curve

Declarations

Ethics approval and consent to participate
The study was approved by the Mansoura Faculty of Medicine Institutional Research Board (approved Proposal Code:R.19.03.441.R1/2019). Informed consents were obtained from all patients.

Consent for publication
Informed consents for publication were obtained from all patients.

Competing interests
The authors declare that they have no competing interests.

Author details
[1]Department of Diagnostic Radiology, Student Hospital Mansoura University, Mansoura, Egypt. [2]Department of Diagnostic Radiology, Faculty of Medicine, Port Said University, 23-Dec, Al Zehour, Al Manakh, Port Said 42511, Egypt. [3]Department of Obstetrics and Gynecology, Faculty of Medicine, Mansoura University, Mansoura, Egypt. [4]Department of Diagnostic Radiology, Faculty of Medicine, Kafr El-Sheikh University, Kafr El-Sheikh, Egypt.

References
1. Torchen LC (2019) Early phenotypes in polycystic ovary syndrome: some answers, more questions. Fertil Steril 111:266–267
2. Sahu A, Tripathy P, Mohanty J et al (2019) Doppler analysis of ovarian stromal blood flow changes after treatment with metformin versus Ethinyl estradiol-cyproterone acetate in women with polycystic ovarian syndrome: a randomized controlled trial. J Gynecol Obstet Hum Reprod 48:335–339
3. Escobar-Morreale HF (2018) Polycystic ovary syndrome: definition, etiology, diagnosis, and treatment. Nat Rev Endocrinol 14:270–284
4. Bani Mohammad M, Majdi SA (2017) Polycystic Ovary Syndrome (PCOS), Diagnostic Criteria, and AMH. Asian Pac J Cancer Prev 18:17–21
5. Teede HJ, Misso ML, Costello MF et al (2018) Recommendations from the international evidence-based guideline for the assessment and management of polycystic ovary syndrome. Clin Endocrinol 89:251–268
6. Karakas SE (2017) New biomarkers for diagnosis and management of polycystic ovary syndrome. Clin Chim Acta 471:248–253
7. Bozdag G, Mumusoglu S, Zengin D et al (2016) The prevalence and phenotypic features of polycystic ovary syndrome: a systematic review and meta-analysis. Hum Reprod 31:2841–2855
8. Lizneva D, Kirubakaran R, Mykhalchenko K et al (2016) Phenotypes and body mass in women with polycystic ovary syndrome identified in referral versus unselected populations: systematic review and meta-analysis. Fertil Steril 106:1510-1520.e2
9. Wiweko B, Indra I, Susanto C et al (2018) The correlation between serum AMH and HOMA-IR among PCOS phenotypes. BMC Res Notes 11:114
10. Abdel Razek A, Abou EH (2021) Differentiation between phenotypes of polycystic ovarian syndrome with songraphy. J Diagn Med Sonogr 37:337–344
11. Gleicher N, Kushnir VA, Darmon SK et al (2018) Suspected ontogeny of a recently described hypo-androgenic PCOS-like phenotype with advancing age. Endocrine 59:661–676
12. Cela V, Obino MER, Alberga Y et al (2018) Ovarian response to controlled ovarian stimulation in women with different polycystic ovary syndrome phenotypes. Gynecol Endocrinol 34:518–523
13. O'Reilly MW, Taylor AE, Crabtree NJ, Hughes BA, Capper F et al (2014) Hyperandrogenemia predicts metabolic phenotype in polycystic ovary syndrome: the utility of serum androstenedione. J Clin Endocrinol Metab 99:1027–1036
14. Yuan C, Liu X, Mao Y, Diao F, Cui Y, Liu J (2016) Polycystic ovary syndrome patients with high BMI tend to have functional disorders of androgen excess: a prospective study. J Biomed Res 30:197–202
15. Zhu RY, Wong YC, Yong EL (2016) Sonographic evaluation of polycystic ovaries. Best Pract Res Clin Obstet Gynaecol 37:25–37
16. Youngster M, Ward VL, Blood EA et al (2014) Utility of ultrasound in the diagnosis of polycystic ovary syndrome in adolescents. Fertil Steril 102:1432–1438
17. Kim HJ, Adams JM, Gudmundsson JA et al (2017) Polycystic ovary morphology: age-based ultrasound criteria. Fertil Steril 108:548–553
18. Rackow BW, Vanden Brink H, Hammers L et al (2018) Ovarian morphology by transabdominal ultrasound correlates with reproductive and metabolic disturbance in adolescents with PCOS. J Adolesc Health 62:288–293
19. Reid SP, Kao CN, Pasch L et al (2017) Ovarian morphology is associated with insulin resistance in women with polycystic ovary syndrome: a cross-sectional study. Fertil Res Pract 3:8
20. Christ JP, Gunning MN, Fauser BCJM (2017) Implications of the 2014 Androgen Excess and Polycystic Ovary Syndrome Society guidelines on polycystic ovarian morphology for polycystic ovary syndrome diagnosis. Reprod Biomed 35:480–483
21. Sipahi M, Tokgöz VY, Keskin Ö et al (2019) Is ovarian volume a good predictor to determine metabolic syndrome development in polycystic ovary patients. J Obstet Gynaecol 2019:1–5.
22. Dewailly D, Lujan ME, Carmina E et al (2014) Definition and significance of polycystic ovarian morphology: a task force report from the Androgen Excess and Polycystic Ovary Syndrome Society. Hum Reprod Update 20:334–352
23. Han YS, Lee AR, Song HK et al (2017) Ovarian volume in Korean women with polycystic ovary syndrome and its related factors. J Menopausal Med 23:25–31
24. Lie Fong S, Laven JSE, Duhamel A et al (2017) Polycystic ovarian morphology and the diagnosis of polycystic ovary syndrome: redefining threshold levels for follicle count and serum anti-Müllerian hormone using cluster analysis. Hum Reprod 32:1723–1731
25. Kenigsberg LE, Agarwal C, Sin S et al (2015) Clinical utility of magnetic resonance imaging and ultrasonography for diagnosis of polycystic ovary syndrome in adolescent girls. Fertil Steril 104:1302–1309
26. Witchel SF, Oberfield S, Rosenfield RL et al (2015) The diagnosis of polycystic ovary syndrome during adolescence. Horm Res Paediatr 83:376–389
27. Fondin M, Rachas A, Huynh V, Franchi-Abella S, Teglas JP, Duranteau L et al (2017) Polycystic ovary syndrome in adolescents: Which MR imaging-based diagnostic criteria? Radiology 285:961–970
28. Samanci C, Alis DE, Ustabasioglu FE, Ozmen E, Ucar AK, Aslan M et al (2017) Apparent diffusion coefficient measurement of ovarian stroma: a potential tool for the diagnosis of polycystic ovary syndrome. Diagn Interv Imaging 98:57–61
29. Razek AAKA, Talaat M, El-Serougy L et al (2019) Clinical applications of arterial spin labeling in brain tumors. J Comput Assist Tomogr 94:1291–1298
30. Abdel Razek AAK, Nada N (2018) Arterial spin labeling perfusion-weighted MR imaging: correlation of tumor blood flow with pathological degree of tumor differentiation, clinical stage and nodal metastasis of head and neck squamous cell carcinoma. Eur Arch Otorhinolaryngol 275:1301–1307

31. Rotterdam ESHRE/ASRM-Sponsored PCOS Consensus Workshop Group Revised (2003) Consensus on diagnostic criteria and long-term health risks related to polycystic ovary syndrome. Fertil Steril 2004(81):19–25
32. Ozkok S, Sorkun M, Dogan MB, Can B, Hocaoglu M, Aslan A (2022) Intravoxel incoherent motion magnetic resonance imaging and derived parameters in the assessment for polycystic ovary syndrome. Egypt J Radiol Nuclear Med 53(1):218
33. Loverro G, Vicino M, Lorusso F et al (2001) Polycystic ovary syndrome: relationship between insulin sensitivity, sex hormone levels and ovarian stromal blood flow. Gynecol Endocrinol 15:142–149
34. Ozdemir O, Sari ME, Kalkan D, Koc EM, Ozdemir S, Atalay CR (2015) Comprasion of ovarian stromal blood flow measured by color Doppler ultrasonography in polycystic ovary syndrome patients and healthy women with ultrasonographic evidence of polycystic. Gynecol Endocrinol 31:322–326
35. Thomassin-Naggara I, Siles P, Balvay D, Cuenod CA, Carette MF, Bazot M (2013) MR perfusion for pelvic female imaging. Diagn Interv Imaging 94:1291–1298
36. Erdem CZ, Bayar U, Erdem LO, Barut A, Gundogdu S, Kaya E (2004) Polycystic ovary syndrome: dynamic contrast-enhanced ovary MR imaging. Eur J Radiol 51:48–53
37. Eissa L, Abdel Razek AAK, Helmy E (2021) Arterial spin labeling and diffusion-weighted MR imaging: Utility in differentiating idiopathic orbital inflammatory pseudotumor from orbital lymphoma. Clin Imaging 71:63–68
38. Abdel Razek AAK, Baky KA, Helmy E (2022) Diffusion tensor imaging in characterization of mediastinal lymphadenopathy. Acad Radiol 29(Suppl 2):S165–S172
39. Abdel Razek AAK, Helmy EM (2021) Differentiation malignant from benign parotid tumors in children with diffusion-weighted MR imaging. Oral Radiol 37(3):463–468
40. Papachroni KK, Piperi C, Levidou G, Korkolopoulou P, Pawelczyk L, Diamanti-Kandarakis E et al (2010) Lysyl oxidase interacts with AGE signalling to modulate collagen synthesis in polycystic ovarian tissue. J Cell Mol Med 14:2460–2469
41. Aoyagi T, Shuto K, Okazumi S, Hayano K, Satoh A, Saitoh H et al (2012) Apparent diffusion coefficient correlation with oesophageal tumour stroma and angiogenesis. Eur Radiol 22:1172–1177
42. Huang Z, Meng X, Xiu J, Xu X, Bi L, Zhang J et al (2014) MR imaging in hepatocellular carcinoma: correlations between MRI features and molecular marker VEGF. Med Oncol 31:313
43. Wang WQ, Chu GH, Hou XX (2023) A comparison of Doppler measures of ovarian blood flow between women with and without ovarian dysfunction and correlations of Doppler indices with ovarian dysfunction markers: a meta-analysis. Ann Transl Med 11(2):110
44. Abdel Razek AA, Samir S, Ashmalla GA (2017) Characterization of parotid tumors with dynamic susceptibility contrast perfusion-weighted magnetic resonance imaging and diffusion-weighted MR imaging. J Comput Assist Tomogr 41:131–136

Publisher's Note